PAN
ARCHIVES OF ACOUSTICS
Vol. **46**, No. 1, pp. 25–30 (2021)
DOI: 10.24425/aoa.2021.136557

Research Paper

SAW Sensor with Langmuir-Blodgett Layer for Detection of Benzene and its Derivatives

Andrzej BALCERZAK*, Piotr KIEŁCZYŃSKI, Marek SZALEWSKI, Krzysztof WIEJA

Institute of Fundamental Technological Research
Polish Academy of Science
Pawińskiego 5B, 02-106 Warsaw, Poland
*Corresponding Author e-mail: abalcerz@ippt.pan.pl

(*received August 4, 2020; accepted October 29, 2020*)

Vapors of benzene and its derivatives are harmful and toxic for human beings and natural environment. Their detection has fundamental importance. For this purpose authors propose surface acoustic wave (SAW) sensor with skeletonized layer deposited by Langmuir-Blodgett (L-B) method. This layer was obtained by depositing a binary equimolar mixture of 5-[[1,3-dioxo-3-[4-(1-oxooctadecyl) phenyl]propyl]amino]–1,3–benzenedicarboxylic acid with cetylamine. The skeletonized sensor layer has been obtained by removing cetylamine. Response of this sensor depends mainly of the electrical dipole momentum of molecule. Among the tested compounds, benzene has a zero dipole moment and gives the smallest sensor response, and nitrobenzene has the largest dipole moment and the sensor reacts most strongly to its vapor.

Keywords: SAW sensor; Langmuir-Blodget layer; vapors; benzene; benzene derivatives.

1. Introduction

Benzene and its derivatives are widely used as synthesis substrates in the organic, pharmaceutical and plastics industry for the production of e.g. synthetic fibers, dyes, drugs, detergents, pesticides, explosives, as well as for the preparation of aniline, phenol and acetone. Both benzene and its derivatives are toxic compounds, which causes the determination of standards related to exposure to them, e.g. the U.S. Occupational Safety and Health Administration has set a permissible exposure limit of 1 part of benzene per million parts of air (1 ppm) in the workplace during an 8-hour workday, 40-hour workweek. The short term exposure limit for airborne benzene is 5 ppm for 15 minutes (U.S. Occupational Safety and Health Administration [OSHA], 2011). Inhaling their vapors in low to moderate levels can cause tiredness, confusion, weakness, drunken-type actions, memory loss, nausea, loss of appetite, hearing loss, and color vision loss. Inhaling high levels aromatic hydrocarbons in a short time may cause light-headedness, nausea, or sleepiness, unconsciousness, acute myeloid leukemia, aplastic anemia, myelodysplastic syndrome, acute lymphoblastic leukemia, and chronic myeloid leukemia and even death (Jameson *et al.*, 2018; Bard *et al.*, 2014; Canadian Centre for Occupational Health and Safety [CCOHS], Agency for Toxic Substances and Disease Registry [ATSDR], 2016; Aransiola *et al.*, 2013). Some of them cause carcinogenicity, especially benzene and nitrobenzene (Smith, 2010; Huff, 2007; National Institute for Occupational Safety and Health [NIOSH]). The ability to detect the presence of benzene vapors and its derivatives is very important for human safety and environmental protection. A leak or other defect in installations using benzene and its derivatives is difficult to eliminate and causes environmental pollution. The vapors of these compounds are flammable and explosive and can cause fires and major infrastructure damage, e.g. for toluene often used as a solvent lower and upper explosive limits with air are 1.3% and 7% by volume, respectively (American Chemistry Council [ACC], 2008).

The relatively high vapor pressures of the abovementioned compounds cause a rapid increase in their vapor concentration in the air. Various methods can be used to detect the presence of these vapors.

Currently used methods, e.g. gas chromatography or mass spectroscopy, achieve high accuracy of determinations, but are used outside of potential hazards, require sample transport and a significant amount of time to perform the measurement.

Another option, which is more desirable because of the quick on-line measurement in the place of potential threat, is the use of an appropriate sensor (Ballantine *et al.*, 1997).

Until now, sensors have been proposed for detecting and measuring the concentration of benzene vapors and their derivatives using QCM sensors with an organometallic layer (Ma *et al.*, 2020) with a polymer layer (Im *et al.*, 2016), resistive-based gas sensors (Mirzaei *et al.*, 2018), gold nanoparticle (Saha *et al.*, 2012), thin layer oxidation reaction (Ke *et al.*, 2009).

For detecting and measuring the concentration of benzene and their derivatives – mainly toluene and xylene, surface acoustic wave (SAW) sensors with cyclodextrin (Dickert *et al.*, 1998) and with polymer layers (Stahl *et al.*, 2018; Panneerselvam *et al.*, 2018) are also being tested.

As mentioned above, benzene derivatives, particularly dangerous for humans and the environment include chlorobenzene and nitrobenzene, for which, according to the authors' knowledge, appropriate sensors have not yet been built. In order to solve this problem, the authors propose the use of an appropriate layer applied on the SAW substrate by the Langmuir-Blodgett (L-B) method.

The Langmuir-Blodgett method (L-B) will allow the production and application of monomolecular layers on substrates. This causes a low mass load of the sensor substrate while maintaining its sensitivity through appropriate selection of the layer and its structure (Kang *et al.*, 2001). In addition, this method allows obtaining monomolecular layers on the SAW substrate in strictly maintained order. Hydrophobic and hydrophilic interactions with the water layer of the particles deposited on the substrate allow such orientation of the molecule that its moiety is available for interaction with the analyte. The thickness of the layer is carefully controlled (Holcroft, Roberts, 1998; Knoll, Rigoberto, 2011).

The purpose of the work is to fabricate a new SAW sensor, which uses waveguides covered on its surface with a specialized Langmuir-Blodgett (L-B) layer as a sensing coating. This configuration of the sensor can provide a reasonable sensitivity to detect benzene vapors and its derivatives – toluene, o-xylene, chlorobenzene and nitrobenzene. These compounds belong to the group of aromatic hydrocarbons and their molecules consist of a benzene ring with various substituents.

The specialized L-B layer has a skeletonized structure with small holes of molecular dimensions.

2. Materials and methods

2.1. Chemicals

5-[[1,3-dioxo-3-[4-(1-oxooctadecyl)phenyl]propyl]amino]-1,3-benzenedicarboxylic acid (DA) was synthesized via hydrogenation (at three atmospheres pressure) of 5-[2-(p-nitrobenzoyl)acetamido]isophthalic acid in ethanol over Reney nickel and subsequent condensation of resulting amine with stearoylchloride in pyridine. The final product was purified by crystallization in acetic acid. Cetylamine (CA) was used as received (Aldrich) (Zhavnerko *et al.*, 1997).

2.2. AFM analysis

Atomic Force Microscopy (AFM) images were obtained with a Nanoscope IIIa (Digital Instruments, USA). The device was equipped with <E> calibrated scanner. AFM images were obtained by tapping mode (TM). Tapping silicon cantilevers with resonance frequency ~300 kHz (Veeco NanoProbe Tips, RTESP) were used for TM regime. Height images are flattened to remove background slopes. No other filtering procedures are performed on these images.

2.3. Langmuir-Blodgett film deposition

The aqueous solution (0.5 mM) of cobalt(II) bromide ($CoBr_2$) in twice-distilled water (pH 5.8) was used as a subphase for monolayer formation and film deposition. Acetone-chloroform (1:1, v:v) solutions (0.5–0.6 mM) were used for spreading of equimolar mixture of DA and CA. To enable a solvent to evaporate completely the compression was started 10 min after spreading.

"Horizontal precipitation" (HP) method was used, where the monolayer is transferred onto a substrate by decreasing of the level of the subphase surface below horizontally kept substrate, which was immersed into the subphase before spreading of DA and CA. The monolayer film was compressed to a "solid" state up to a surface pressure of 30 mN/m. Then the water was allowed to slip off slowly (0.5–0.6 ml/min) from the substrate surface leaving a homogeneous monolayer film on the substrate. A waveguide surface of the reference line was protected against film deposition by a tape. The surface pressure was changed slightly (less then 1–2 mN/m) during a deposition process. Z-type film is formed in the case of HP deposition. The AFM image of the layer is presented in Fig. 1.

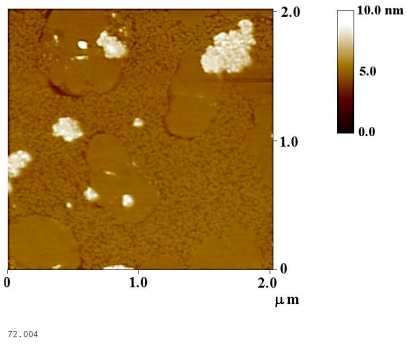

Fig. 1. The AFM image of DA+CA layer.

The presence of $CoBr_2$ causes a modification of the layer structure by the formations of salts and 1,3-

diketonate complexes of DA with Co^{2+}, what makes this layer very stable due to intermolecular interactions between DA molecules.

Subsequently, the cetylamine was removed from the layer by washing of the film in chloroform. This process caused the formation of the structure containing into a tilted phase presumable pores of the molecular dimensions with diameter distribution from 16 nm up to 0.2 nm, which modified properties of the sensing layer. The AFM image of the porous, skeletonized layer is presented in Fig. 2 and section analysis of this layer in Fig. 3.

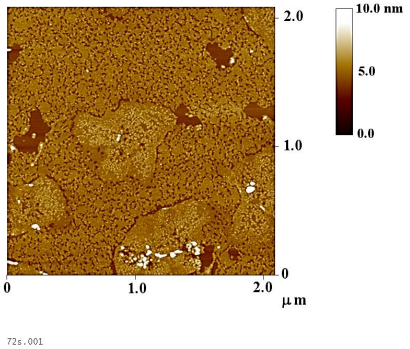

Fig. 2. The AFM image of DA skeletonized layer.

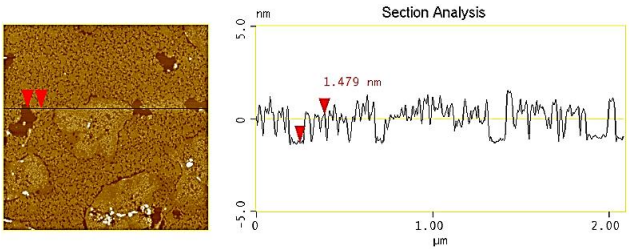

Fig. 3. Section analysis of DA skeletonized layer.

2.4. Experimental set-up and measurement procedure

The experimental set-up consists of the SAW sensor delay line, chamber, electronic module, power supply, A/D converter and PC computer with specialized software. This set-up is based on frequency changes in an acoustic surface wave dual delay line system. The substrate is made from Y-Z lithium niobiate and has interdigital transducers forming two independent and identical acoustic delay lines. A part of surface of one delay line is covered by monomolecular chemosensitive layer and forms the measurement line. Second delay line is the reference line for a temperature and pressure compensations. The role of electronic module is to generate ultrasonic waves in both delay lines and to determine the difference frequency. The initial operating frequency of both lines equals 70.3 MHz, but the difference frequency appears after covering one delay line by chemosensitive layer. Both lines are parts of the positive feedback loop of oscillator circuits. The generation and stabilization circuits for both lines are identical. The response to the presence of vapors of benzene and its derivative in air is detected and recorded as a change of the difference frequency between the two oscillator frequencies. The accuracy of difference frequency measurements by electronic module equals 1 Hz. The sensor delay line is thermally coupled with a heating element. The scheme of the measuring set up is presented in Fig. 4.

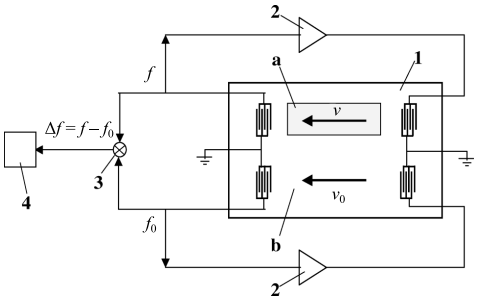

Fig. 4. The scheme of the measuring set up. 1 – sensor delay line (a – measuring channel, b – reference channel), 2 – high frequency amplifier, 3 – balanced mixer, 4 – difference frequency recorder.

3. Measurements and calculations

When the working conditions of the sensor delay line were stabilized (a constant value of the differential frequency, and temperature 35.00 ± 0.05°C), the mixture of air and the vapors of the benzene and its derivatives at 300 ppm concentration was pumped into the chamber. In the two-second intervals of time, the response of the delay line was recorded as the dependence of the differential frequency on time. Additionally, the temperature in the chamber is also recorded. Benzene, toluene, o-xylene, chlorobenzene and nitrobenzene have been chosen as tested liquids. After 20 minutes the chamber was filled by clean air. In the two-second intervals of time, the response of the sensor was recorded continuously as the dependence of the difference frequency on time by data acquisition set-up.

In Figs 5–9, the representative plots of the differential frequency are presented as the result of influence of the air containing 300 ppm of benzene, toluene, o-xylene, chlorobenzene and nitrobenzene, on the sensor

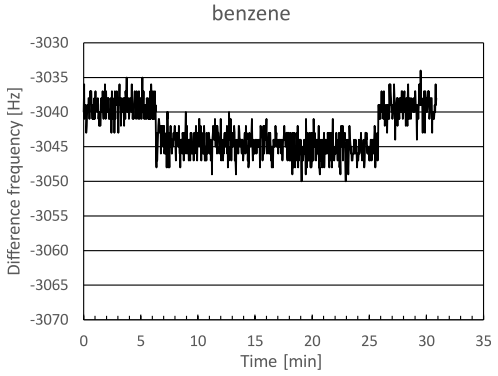

Fig. 5. Interaction of the sensor layer with benzene vapors in the air at a concentration of 300 ppm.

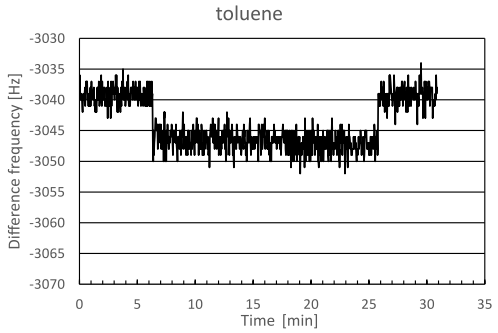

Fig. 6. Interaction of the sensor layer with toluene vapors in the air at a concentration of 300 ppm.

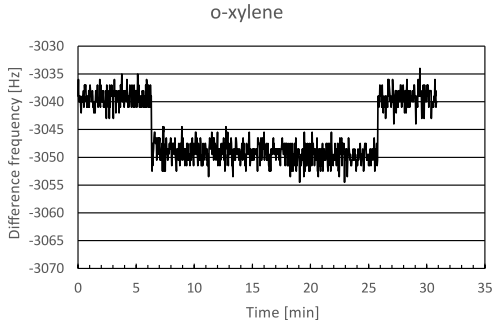

Fig. 7. Interaction of the sensor layer with o-xylene vapors in the air at a concentration of 300 ppm.

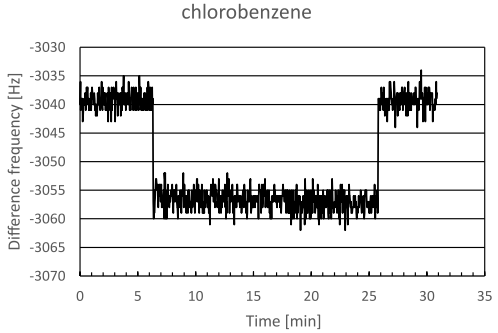

Fig. 8. Interaction of the sensor layer with chlorobenzene vapors in the air at a concentration of 300 ppm.

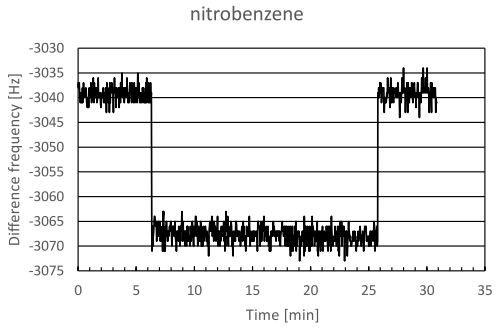

Fig. 9. Interaction of the sensor layer with nitrobenzene vapors in the air at a concentration of 300 ppm.

layer. Table 1 contains values of the response parameter of the sensor with DA nanolayer on the presence of tested vapors. After removing the vapor of analite by fresh air the difference frequency return to initial values.

Table 1. Decrease of difference frequency after contact with vapor of the dual delay line covered by porous DA layer on the presence vapors of benzene and its derivatives.

Name	Decrease of difference frequency after contact with vapor [Hz]
benzene	6
toluene	8
o-xylene	10
chlorobenzene	17
nitrobenzene	28

Given the relationship between the change in the differential frequency Δf measured as the sensor response to the change in mass Δm of its chemosensitive layer through the interaction of the tested molecules with the layer (Ballantine *et al.*, 1997):

$$\Delta f = -K f_0^2 \frac{\Delta m}{A}, \tag{1}$$

(where K is a constant for Y-Z lithium niobiate $K = 5.5 \cdot 10^{-11}$ s$\cdot$m^{2}g^{-1} (Slobodnik, Conway, 1970), f_0 – operating frequency of the sensor and A is a surface of sensing layer) the number of bonded molecules N_B per surface of sensing layer can be obtained:

$$\frac{N_B}{A} = -\frac{\Delta f N_A}{K f_0^2 M}, \tag{2}$$

where N_A and M are Avogadro's number and molecular mass, respectively.

The result of calculation are placed in Table 2.

Table 2. Number of molecules per surface of sensing layer.

Name	Number of molecules per surface of sensing layer [10^{17} molecules/m^2]
benzene	1.70
toluene	1.92
o-xylene	2.09
chlorobenzene	3.44
nitrobenzene	5.04

4. Discussion of results

The large number of nitrobenzene molecules bound to the layer is very clearly visible. To explain this observation, the van der Waals volume of the studied molecules and their dipole moments were taken into account – Table 3.

Taking account the fairly obvious parameter for the porous layer, i.e. van der Waals volume, the volume of chlorobenzene, and especially nitrobenzene, do not differ much from other benzene derivatives, i.e. toluene and o-xylene.

Table 3. Molecular properties of benzene and its derivatives.

Name	Van der Waals' volume [10^{-30} m^3/molecule] (Smallwood, 2012)	Electrical dipole moment [10^{-30} C · m] (Smallwood, 2012)
benzene	80.4	0.0
toluene	98.8	1.3
o-xylene	117	1.5
chlorobenzene	96	5.2
nitrobenzene	103	14.3

The situation is different with the dipole moment of the aromatic hydrocarbons tested. Nitrobenzene dipole moment has a much higher value than other benzene derivatives. This may explain greater ability of nitrobenzene molecules to adsorb on the chemosensitive layer than the other molecules tested (Table 2).

5. Conclusions

1) The proposed L-B layer having skeletonized structure with small holes of molecular dimensions on the SAW substrate enables detection of benzene vapors and its derivatives - toluene, o-xylene, chlorobenzene and nitrobenzene.
2) The decrease in differential frequency is associated with the dipole moment of the analyte molecule. Van der Waals volume plays a smaller role.
3) After removing the analyte, the differential frequency returns to the initial value.
4) The highest sensor response occurs for nitrobenzene, followed by chlorobenzene – the most toxic benzene derivatives.

References

1. Agency for Toxic Substances and Disease Registry (2016), *Toluene Toxicity Physiologic Effects*, pp. 10–12.
2. American Chemistry Council (2008), *Working with Modern Hydrocarbon and Oxygenated Solvents: A Guide to Flammability*, American Chemistry Council, Solvents Industry Group, Wrlington USA.
3. Aransiola E.F., Daramola M.O., Ojumu T.V. (2013), *Xylenes: production technologies and uses*, *Xylenes: Synthesis, Characterization and Physicochemical Properties – Chemical Engineering Methods and Technology*, Nova Science Publishers, 1–12.
4. Ballantine D.S. *et al.* (1997), *Acoustic Wave Sensors*, Academic Press, San Diego.
5. Bard D. *et al.* (2014), Traffic-related air pollution and the onset of myocardial infarction: disclosing benzene as a trigger? A small-area case-crossover study, *Plos One*, **9**: 6, doi: 10.1371/journal.pone.0100307.
6. Canadian Centre for Occupational Health and Safety (2018), *Health Effects of Toluene.*
7. Dickert F.L., Forth P., Bulst W.-E., Fischerauer G., Knauer U. (1998), SAW devices-sensitivity enhancement in going from 80 MHz to 1 GHz, *Sensors ana Actuators B: Chemical*, **46**(2): 120–125, doi: 10.1016/S0925-4005(98)00097-5.
8. Holcroft B., Roberts G.G. (1998), Surface acoustic wave sensors incorporating Langmuir-Blodgett films, *Thin Solid Films*, **160**(1–2): 445–452, doi: 10.1016/0040-6090(88)90090-9.
9. Huff J. (2007), Benzene-induced cancers: abridged history and occupational health impact, *International Journal of Occupational and Environmental Health*, **13**(2): 213–221, doi: 10.1179/oeh.2007.13.2.213.
10. Im J., Sterner E.S., Swager T.M. (2016), Integrated Gas Sensing System of SWCNT and Cellulose Polymer Concentrator for Benzene, Toluene, and Xylenes, *Sensors (Basel)*, **16**(2): 183, doi: 10.3390/s1602.
11. Jameson J.L., Fauci A.S., Kasper D.L., Hauser S.L., Longo D.L., Loscalzo J. (2018), *Harrison's Principles of Internal Medicine*, 20th ed., McGraw-Hill Education.
12. Kang K.H., Kim J.M., Kim D.K., Jung S.B., Chang J.S., Kwon Y.S. (2001), Effect of pH on the properties of palmitic acid LB films for gas sensors, *Sensors and Actuators B: Chemical*, **77**(1–2): 293–296, doi: 10.1016/S0925-4005(01)00745-6.
13. Ke M.-T., Mu-Tsun L., Lee C.-Y., Fu L.-M. (2009), A MEMS-based Benzene Gas Sensor with a Self-heating WO3 Sensing Layer, *Sensors (Basel)*, **9**(4): 2895–2906; doi: 10.3390/s90402895.
14. Knoll W. [Ed.], Rigoberto C. (2011), *Functional Polymer Films*, Wiley-VCH.
15. Ma Z. *et al.* (2020), A benzene vapor sensor based on a metal-organic framework-modified quartz crystal microbalance, *Sensors and Actuators B: Chemical*, **311**, 127365, doi: 10.1016/j.snb.2019.127365.
16. Mirzaei A., Kim J.-H., Kim H.W., Kim S.S. (2018), Resistive-based gas sensors for detection of benzene, toluene and xylene (BTX) gases: a review, *Journal of Materials Chemistry C*, **6**(16): 4342–4370, doi: 10.1039/ C8TC00245B.
17. National Institute for Occupational Safety and Health (2018), *Nitrobenzene. Immediately Dangerous to Life and Health Concentrations.*
18. Panneerselvam G., Thirumal V., Pandya H.M. (2018), Review of surface acoustic wave sensors for the detection and identification of toxic environmental gases/vapours, *Archives of Acoustic*, **43**(3): 357–367, doi: 10.24425/123908.
19. Saha K., Agasti S.S., Kim C., Li X., Rotello V.M. (2012), Gold nanoparticles in chemical and biological sensing, *Chemical Review*, **112**(5): 2739–2779; doi: 10.1021/cr2001178.

20. Slobodnik A.J., Conway E.D. (1970), *Microwave Acoustic Handbook. Vol. 1, Surface Wave Velocities*, Bedford, MA: Air Force Cambridge Research Laboratories.

21. Smallwood I. (2012), *Handbook of Organic Solvent Properties*, Butterworth-Heinemann, Oxford.

22. Smith M.T. (2010), Advances in understanding benzene health effects and susceptibility, *Annual Review of Public Health*, **31**: 133–148; doi: 10.1146/annurev.publhealth.012809.103646.

23. Stahl U. *et al.* (2018), Long-term capability of polymer-coated surface transverse wave sensors for distinguishing vapors of similar hydrocarbons, *Sensors and Actuators B: Chemical*, **274**: 560–564, doi: 10.1016/j.snb.2018.08.013.

24. U.S. Occupational Safety and Health Administration (2011), *Chemical Sampling Information Benzene*. Retrieved on 2011-11-23.

25. Zhavnerko G.K., Filippov V.V., Severin F.M., Kuchuk T.A., Agabekov V.E. (1997), Formation and features of skeletonized structures in two-component Langmuir-Blodgett films, *Journal of Colloid and Interface Science*, **193**(1): 1–7, doi: 10.1006/jcis.1997.4872.